2011 50th IEEE Conference on Decision and Control and
European Control Conference (CDC-ECC)
Orlando, FL, USA, December 12-15, 2011

Hybrid vehicle stability system using a HOSM control

S. Delprat and A. Ferreira de Loza

Abstract— **This paper tackles the problem of driving stability for a hybrid vehicle. A rear electric motor has been added to the vehicle and the positive/negative torque generated by this motor affects the driving conditions. The problem of yaw stability control is addressed using a high order sliding modes (HOSM) control for handling the system under uncertain driving conditions. The proposed control can cope against the vehicle uncertainties and external perturbations. The feasibility of this approach was tested in a vehicle simulator.**

I. INTRODUCTION

Recently an intense scientific and technical development for the hybrid vehicle technology has arisen. Hybrid vehicle provides an attractive alternative to reduce fuel consumption and diminish the emissions to the environment. Furthermore, the addition of electrical motors in the driveline provides regenerative braking and electric traction feasibilities. The performance of the system also depends on the suitable control algorithms design. In general two control levels are involved in a hybrid vehicle: an energetic management control for improving the fuel economy and a vehicle stability control for ensuring the system's driveability.

The vehicle mechanical arrangement considered in this work is shown in Fig. 1. The vehicle has two electric machines. The front electric machine has a lower rated power. It may be used as an integrated starter/generator and also can be used to improve the internal combustion (IC) engine fuel consumption. Adopting separate motors at the front and rear wheels axes allows an easy integration of a powerful machine into the rear vehicle axis for pure electric vehicle propelling.

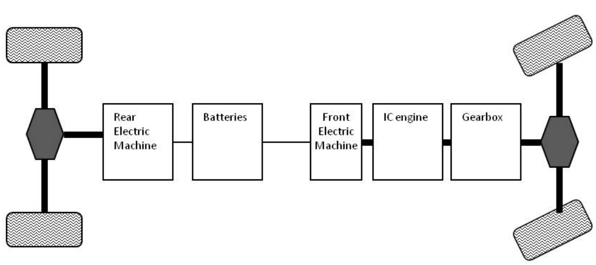

Fig. 1. Vehicle system arrangement

S. Delprat and A. Ferreira de Loza are with Univ. Lille Nord de France, F-59000 Lille, France UVHC, LAMIH, F-59313 Valenciennes, France CNRS, UMR 8530 F-59313 Valenciennes, France sebastien.delprat@univ-valenciennes.fr, alejandra.ferreira@hotmail.com

For ensuring low fuel consumption, the electric machines and the IC engine set point are given by an energetic management (EM) algorithm. This algorithm is basically a robust predictive control law (see [1], [2] and references therein). In the system under study, the energy management control law was designed by VALEO company in collaboration with the university of Valenciennes.

EM strategy is based on a highly simplified vehicle model. The main problem is that for supplying the requested power the electric machine and IC engine operating points are chosen regardless to the vehicle stability, assuming that the driver is able to drive the car along the road whatever the energetic control law do. When there is no rear electric machine, the optimization algorithm works well [2]. Nevertheless, with a rear electric machine, a risk situation occurs if, for example, the driver enters in a curve and the optimization control strategy decides to stop propelling the vehicle using the rear drive and starts propelling the vehicle using the IC engine, while using the rear motor for applying negative torque (i.e. energy recovering issues). In this case, an undesired moment can arise provoking the lost of driveability of the system. Hence, the vehicle stability must be ensured (i.e. the vehicle should turn safety whatever the energetic control decide to do).

In general, vehicle stability control systems which prevent vehicles from spinning and drifting out, have been already developed and commercialized. Such systems are known as electronic stability program (ESP) systems [3], [4], [5]. The function of these systems is to restore the yaw rate of the vehicle as much as possible to the nominal motion expected, in spite of the road and driving conditions. Most of the ESP strategies act on the vehicle dynamics using the mechanical brakes to generate differential torques on the right and left wheels to produce a yaw moment. However, ESP algorithm acts during "emergencies" (i.e. when driving on the limits of adhesion [3]) and it should not be used during a normal driving situation. Under the considered hybrid vehicle arrangement (Fig. 1), the front/rear EM splitting strategy could generate a yaw moment and therefore the vehicle yaw dynamics may be affected. It should be ensured that ESP algorithm will not be triggered by an improper choice of the front/rear torque.

Considering the aforementioned, in this work the problem of vehicle yaw stability is addressed. The proposed control does not relay in differential braking. This control is used to ensure that the front/rear torque split computed by the energetic management algorithm will not bring the vehicle towards an unstable situation. It does not substitute the ESP algorithm.

TABLE I

NOMENCLATURE

i	wheel $i \in \{1,2\}$
v	velocity at the vehicle CoG
β	vehicle side slip angle
$\dot{\psi}$	yaw rate
F_{xi}	longitudinal friction force on the i-wheel
F_{yi}	lateral friction force on the i-wheel
δ	steering angle
α_i	wheel side slip angle
λ_i	longitudinal slip of the i-wheel
ω_i	wheel angular velocity
$v_{\omega i}$	wheel velocity
ℓ_i	geometry parameter
$L = \sum \ell_i$	geometry parameter
m	vehicle mass
J_ψ	vehicle moment of inertia
J	wheel moment of inertia
C_x	longitudinal wheel stiffness parameter
C_y	cornering wheel stiffness parameter
R	wheel radius
T_i	electric motor torque
T_{IC}	internal combustion motor torque

Vehicle dynamics is influenced by several uncertain conditions (weather, road state, etc.) and perturbations (aerodynamic drag forces, undesirable yaw moments, etc). Sliding modes technique has shown to be an effective strategy to cope against uncertainties and perturbations [6], [7], [8]. Traditional sliding modes control has been already applied in the design of ABS control systems, steering by wire systems, etc. (see [9], [10]). Moreover, high order sliding modes techniques have been successfully applied in the observation of vehicle dynamics (see [11], [12], [13]), as well as in traction control strategies [14]. A high order sliding modes output-feedback control was introduced in [15]. The principal advantage of such controller is that no detailed mathematical model is needed. These kind of controllers can cope with the nonlinearities and uncertainties presented in the vehicle dynamics.

The contribution of this work is the design of a robust control methodology to improve the vehicle handling. The proposed methodology considers an output high order sliding mode controller. The controller do not rely in the exact and detailed knowledge of the system and driving conditions. This control could be integrated as an intermediate layer between the energy optimization management and the ESP layer for guarantee the system driveability.

Paper structure. In the next section the vehicle dynamics is presented. Section III, describes the vehicle tyre-road interaction. A HOSM controller is proposed in Section IV. Section V is devoted to the simulations. Finally conclusions are presented in Section VI.

II. PROBLEM STATEMENT

The variables and parameters used in this manuscript are summarized in Table I and Fig. 2.

Let us consider the nonlinear single-track model [16]. In this model the differences between the right and left wheels are ignored, considering both wheels as a single unit Fig. 2. The yaw dynamics is given by

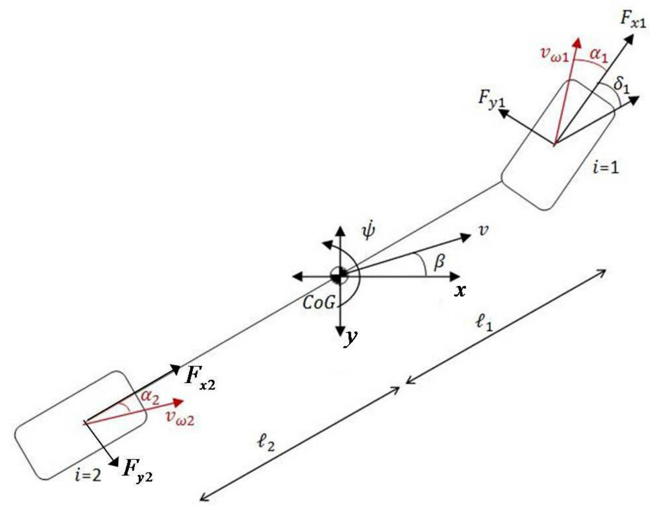

Fig. 2. Vehicle schematic model

$$\ddot{\psi} = \frac{\ell_1}{J_\psi}\cos\delta F_{y1} - \frac{\ell_2}{J_\psi}F_{y2} + \frac{\ell_1}{J_\psi}\sin\delta F_{x1} \quad (1)$$

$$y = \dot{\psi} \quad (2)$$

where y is the measured variable. The available control input is the front longitudinal traction force F_{x1}. Here let us point out that the available actuators for the system presented in Fig. 2 are the front and rear electric motors. However, in the considered model, only the longitudinal traction force F_{x1} is achievable.

Before continuing some assumptions are considered henceforth:

A1. The vehicle velocity $v \neq 0, \quad v \in \left[\, v_{\min} \quad v_{\max} \,\right]$, i.e. we are assuming that the vehicle is traveling at a nominal but unknown velocity.

A2. The yaw controller will be active for $\delta > \delta_m$ with $\delta_m > 0$.

Control goal. The aim of this paper is to design a robust output control for system (1) - (2) such that the output follows a prescribed reference $\dot{\psi}_{des}$, in spite of the uncertain system driving conditions.

The control input F_{x1} results from the interaction between the tyre and the road, see Fig. 4. Hence, for studying the vehicle body dynamics, it is necessary to investigate the tyre/road interface.

III. TYRE-ROAD INTERFACE

Let us consider the rotational dynamics in the front wheel (see Fig. 3)

$$J\dot{\omega}_1 = -RF_{x1} + T_T \quad (3)$$

where the T_T is the total torque applied to the front axis. This torque comes from the internal combustion engine torque T_{IC} and the electric motor torque T_1, i.e.

$$T_T = T_{IC} + T_1 \quad (4)$$

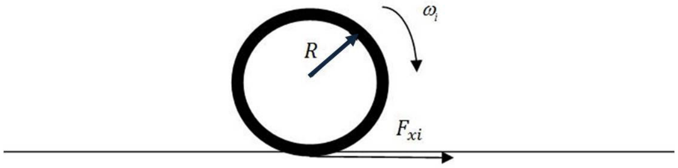

Fig. 3. Wheel Dynamics

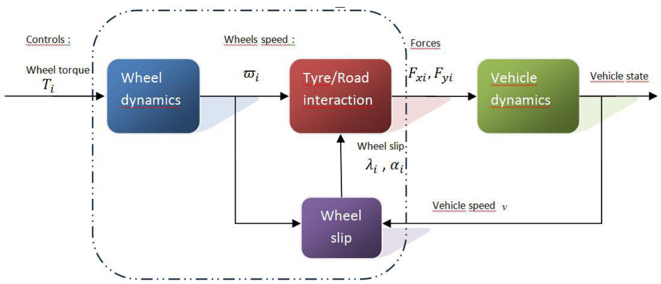

Fig. 4. Vehicle forces interactions

The longitudinal traction force F_{x1}, is a nonlinear function of wheel slip λ_1 and the longitudinal wheel stiffness C_x, the friction coefficient, temperature, etc. The values of $F_{xi} = f(C_{xi}, \lambda_i)$ are obtained experimentally for different types of surface and weather conditions. Fig. 5 shows typical $\lambda - F_x$ curve. Although, in nominal driving conditions, the values of the slip λ_i are small and the following expression holds

$$F_{xi} = C_x \lambda_i \tag{5}$$

In the literature, different wheel slip λ_i definitions are considered (see the corresponding chapter in [3]). Here, the longitudinal wheel slip is consider as

$$\lambda_i = \frac{\omega_i R - v_{\omega xi}}{\omega_i R} \qquad \omega_i R > v_{\omega xi} \quad \omega_i \neq 0 \; accelerating \tag{6}$$

where $v_{\omega xi}$ is the projection of the wheel velocity on the $x - axis$ direction.

Differentiating (6), the slip ratio dynamics is given by

$$\dot{\lambda}_i = -\frac{v_{\omega xi}}{J\omega_i^2} F_{xi} + \frac{v_{\omega xi}}{JR\omega_i^2} T_i - \frac{\dot{v}_{\omega xi}}{R\omega_i} \tag{7}$$

Taking into account expressions (1), (5) and (7), we have

$$\ddot{\psi} = \frac{\ell_1}{J_\psi} \cos\delta F_{y1} - \frac{\ell_2}{J_\psi} F_{y2} + \frac{\ell_1 C_x}{J_\psi} \sin\delta \lambda_1 \tag{8}$$

$$\dot{\lambda}_1 = -\frac{C_x v_{\omega x1}}{J\omega_1^2} \lambda_1 - \frac{\dot{v}_{\omega x1}}{R\omega_1} + \frac{v_{\omega x1}}{JR\omega_1^2} T_1 \tag{9}$$

$$y = \dot{\psi} \tag{10}$$

The above equations represent a highly uncertain system, which is affected by unmeasurable variables $\beta, v_{\omega x1}$, F_{yi}, etc. and uncertainties such as C_x, R, J_ψ, J, etc. The only available output is the yaw rate $\dot{\psi}$.

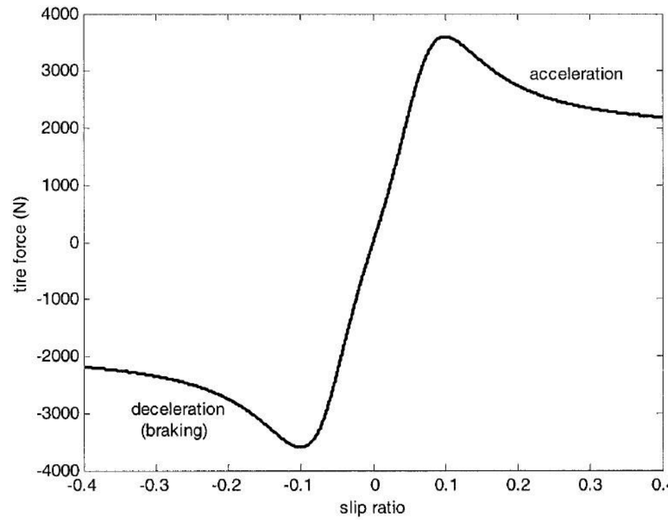

Fig. 5. Longitudinal tire force as a function of slip ratio

The dynamic of the tyre-wheel interface given in (7) has a steady-state dynamics then, except for the transient behavior of the higher derivatives, let us assume

A3. The forces produced by the wheels as well as its successive derivatives until the order r are bounded $|F_{xi}| < f^+, |F_{yi}| < f^+$, $\left|F_{xi}^{(r)}\right| < f^+$ and $\left|F_{yi}^{(r)}\right| < f^+$

The solutions of the discontinuous differential equations are understood in the Filippov's sense [17].

IV. HIGH ORDER SLIDING MODE CONTROLLER

Let us define

$$\sigma := \dot{\psi} - \dot{\psi}_{des}$$

with $\dot{\psi}_{des}$ a sufficiently smooth function. The task is to achieve $\sigma \equiv 0$ using only the output information. The HOSM methodology is a good selection for designing a control without paying attention in the detailed mathematical model of the system.

The system under consideration (8)-(10) has a constant and known relative degree $r = 2$, i.e. taking the successive derivatives of σ along the time, we have

$$\sigma^{(2)} = h + gu \tag{11}$$

where

$$\begin{aligned} h &= \frac{\ell_1}{J_\psi}\Big(\dot{\delta}\left(\cos\delta F_{x1} - \sin\delta F_{y1}\right) + \cos\delta \dot{F}_{y1} - \frac{\ell_2}{\ell_1}\dot{F}_{y2} \\ &\quad + \ddot{\psi}_{des} + \sin\delta \dot{F}_{x1} + \cos\delta F_{x1}\Big) \\ g &= \frac{\ell_1 C_x v_{\omega x1}}{J_\psi J R \omega_1^2} \sin\delta \end{aligned}$$

the control input $u = T_1$. For constructing a HOSM controller, some assumptions regarding to the boundness of the system, must be done.

Considering $A3$ and a constant $H > 0$, it can be shown that

$$
\begin{aligned}
|h| &\leq \frac{2L}{J_\psi}\left(\left|\dot{\delta}\right| f^+ + 2f^+\right) \leq H & (12)\\
|g| &\leq \left|\frac{\ell_1 C_x v_{\omega x1}}{J_\psi J R \omega_1^2}\right| \\
&\leq \left|\frac{\ell_1 C_x}{J_\psi J R}\frac{1}{\omega_1}\right| & (13)
\end{aligned}
$$

Then, due to $A1$ and considering (6) we can assume $\omega \in [\ \omega_m \quad \omega_M\ ]$. For some $G_m, G_M > 0$, $\frac{\ell_1 C_x}{J_\psi J R}\left|\frac{1}{\omega_{1m}}\right| < G_M$, $G_m < \frac{\ell_1 C_x}{J_\psi J R}\left|\frac{1}{\omega_{1M}}\right|$. Thus $G_m \leq |g| \leq G_M$ and due to A2 $g \neq 0$. Then, following [15], the next differential inclusion is implied

$$
\sigma^{(2)} \in [-H, H] + [G_m, G_M]\, u \tag{14}
$$

and a second order control law

$$
u = -\Gamma \operatorname{sign}\left(\dot{\sigma} + |\sigma|^{1/2} \operatorname{sign}(\sigma)\right) \tag{15}
$$

where Γ is related with the boundness of the system which satisfy (14). Selecting $\Gamma > H$ leads to the establishment of a $2nd - sliding$ mode $\sigma \equiv 0$ attracting each trajectory in finite time. In [15], was shown that the above controller is insensitive to any disturbance which keeps (14) and the relative degree r.

The proposed control (15) is discontinuous. In order to smooth the control action two different approaches can be followed. The first approach is to increase the order of the HOSM controller maintaining the relative degree of the system in $r = 2$ and then apply and integrator to smooth the signal. This implies to find the bounds of $\sigma^{(3)}$ which can be achieved after a tiresome computation. A second alternative is to suppose that the relative degree of the system is one. It can be done if we assume that the dynamics of the tyre-road interface is stable and fast. In fact, as the controller will be working in the linear region of the $\lambda - F_x$, we can neglect the tyre-road dynamics. In [18] was shown that HOSM controllers are robust to the presence of unaccounted actuators dynamics. Then the control action is given by

$$
\begin{aligned}
u &= u_1 & (16)\\
\dot{u}_1 &= -\Gamma \operatorname{sign}\left(\dot{\sigma} + |\sigma|^{1/2} \operatorname{sign}(\sigma)\right) & (17)
\end{aligned}
$$

V. SIMULATIONS

The performance of the designed controller was proved in the PROSPER/CALLAS 4.9 simulator developed by OKTAL. The vehicle parameters are listed in Table II. The sampling time was $\tau = 1[ms]$ and the Euler integration method was used for simulations. During the experiment a regenerative braking (negative torque) is carried by the rear motor (due to the external energetic algorithm management) while the vehicle is turning.

The control objective is that the vehicle follows a desired yaw rate $\dot{\psi}_{des}$ defined by the commanded steering angle δ (see Fig. 6). Several yaw rate reference models are proposed in the literature, (see [3], [16]). Here we are considering a simplified yaw rate reference generator. The desired yaw rate which can therefore be obtained from steering angle and assuming conservative values for the velocity v_o and cornering stiffness C_{yi}

$$
\dot{\psi}_{des} = \frac{v_0 \cos\beta}{L + \frac{m(v_o\cos\beta)^2(\ell_2 C_{y2} - \ell_1 C_{y1})}{2C_{y1}C_{y2}L}}\delta
$$

TABLE II

SIMULATION PARAMETERS

ℓ_1	836.8	$[mm]$
ℓ_2	1853.2	$[mm]$
m	1724.5	$[Kg]$
J_ψ	320.22	$[Nm]$
J	0.747	$[Nm]$
C_{y1}	61682	
C_{y2}	59319	
R	0.276	$[m]$
Γ	40	

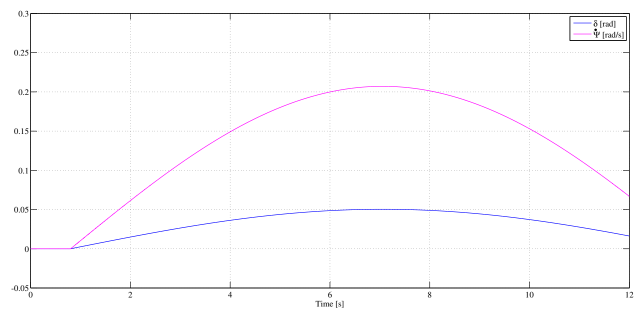

Fig. 6. Vehicle steering angle $\delta\,[rad]$ and desired yaw rate $\dot{\psi}\,[rad/s]$.

The system performance is showed in Fig. 7. Two vehicles are shown. Both of them are under a rear negative torque condition. The vehicle in red has an HOSM stability control and keeps the maneuverability during the experiment. On the contrary, the vehicle without control (in blue) skids.

The Fig. 7 shows the yaw rate tracking for the vehicle with and without HOSM control. The HOSM control maintains the desired yaw rate in spite of the rear negative torque condition. Meanwhile, in the below sketch is seen that the system is unable to follow the reference.

We design a HOSM controller of 2nd order and we apply an integrator to smooth the action on the actuators. The total measured torque in front and rear wheels is depicted in Fig. 11. For obtaining the derivatives of the error $\dot{\sigma}, \sigma^{(2)}$ a HOSM differentiator was used (see [15]). When the differentiator converges, after a finite time $t > 0.1$, the controller is turned on.

The acceleration, velocity and slip angle of the vehicle are depicted in Fig. 9-10 for the system with and without control respectively. Fig. 9 shows that the control action decrease the vehicle velocity. This situation is not desirable from the "driving comfort" point of view, because the effects of the control action may differ from the wishes of the driver. Further studies should be done to find a compromise between the security and driving comfort matters.

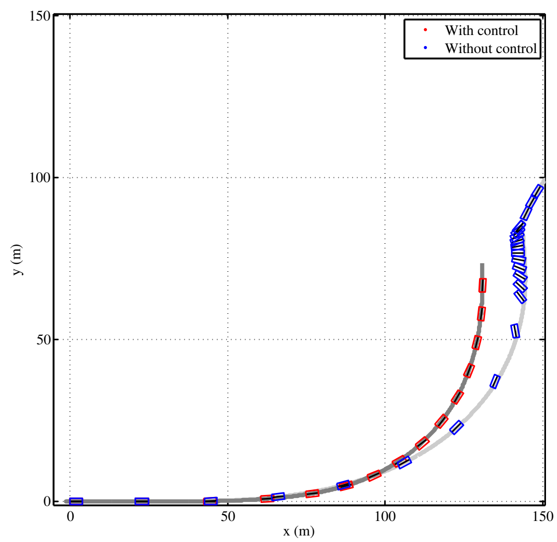

Fig. 7. Vehicle yaw rate tracking with and without control in a negative rear torque condition. The HOSM control successfully maintains the system yaw rate and keeps the vehicle maneuverability.

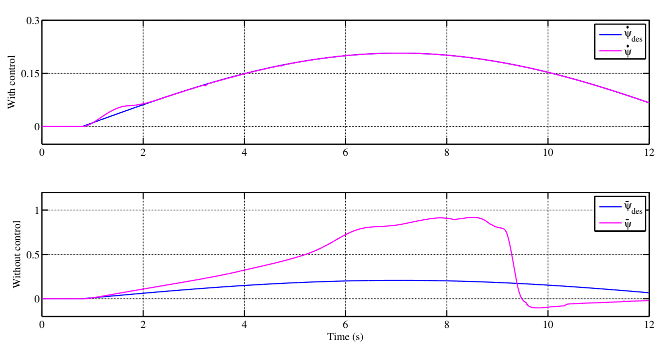

Fig. 8. Vehicle yaw rate tracking with and without control under a negative rear torque situation.

VI. CONCLUSIONS

This work presented a finite time HOSM controller for a new scheme of hybrid vehicles design. The proposed controller guarantees the maneuverability of the vehicle in spite of the unknown conditions provoked by the effects of the rear electric motor. The controller copes against the uncertainties of the system. The feasibility of the proposed scheme was validated in PROSPER/CALLAS 4.9 simulator.

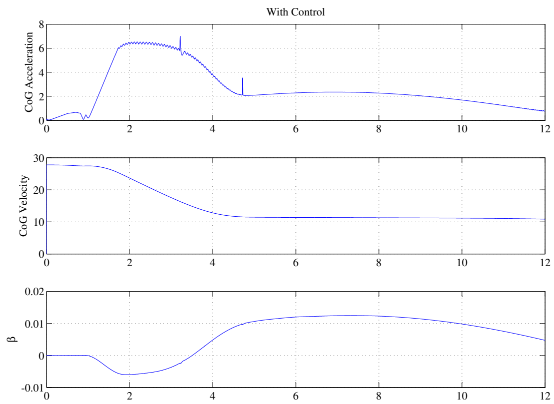

Fig. 9. System variables without the HOSM stability control action. Acceleration $d\nu/dt\left[m/s^2\right]$, Velocity $\nu\,[m/s]$, slip angle $\beta\,[rad]$.

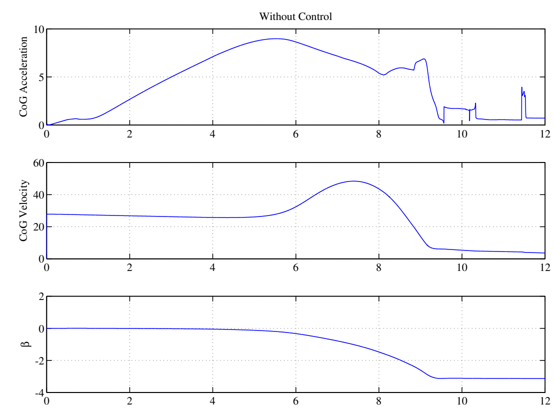

Fig. 10. System variables when the HOSM stability control is applied. Acceleration $d\nu/dt\left[m/s^2\right]$, Velocity $\nu\,[m/s2]$, Slip angle $\beta\,[rad]$.

Further research should be done for improving the driving comfort issue.

VII. ACKNOWLEGEMENTS

The present work has been supported by International Campus on Safety and Intermodality in Transportation, the European Community, the Nord-Pas-de-Calais Delegation for Research and Technology, the French Ministry of Higher Education and Research, and the National Center for Scientific Research (CNRS). This work is also supported by the French Environment and Energy Management Agency (ADEME) through the HYBRELEC project.

REFERENCES

[1] S. Kermani, R. Trigui, S. Delprat, B. Jeanneret, and T. Guerra, "PHIL implementation of energy management optimization for a parallel HEV on a predefined route," *IEEE Transactions on Vehicular Technology*, 2011.

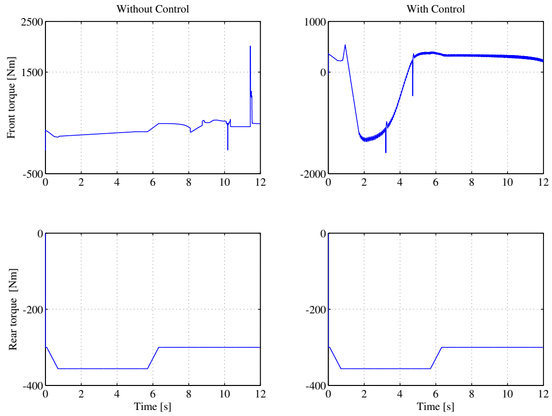

Fig. 11. The total torque applied to the front wheels and rear wheels. A regenerative braking is occurring in the rear wheels.

[2] J. Bernard, S. Delprat, F. Buechi, and T. Guerra, "Fuel efficient power management strategy for fuel cell hybrid powertrains," *Control Engineering Practice*, vol. 18, pp. 408–417, 2010.

[3] R. Rajamani, *Vehicle Dynamics and Control*. Springer Verlag, 2006.

[4] M. Canale, L. Fagiano, A. Ferrara, and C. Vecchio, "Vehicle yaw control via second-order sliding-mode technique," *IEEE Trans. on Industrial Electronics*, vol. 55, pp. 3908–3916, 2008.

[5] J. Tjonnas and T. A. Johansen, "Stabilization of automotive vehicles using active steering and adaptive brake control allocation," *Transactions on Control Systems Technology*, vol. 18, pp. 545–558, 2010.

[6] V. I. Utkin, *Sliding modes in control and optimization*. Berlin, Germany: Springer Verlag, 1992.

[7] V. I. Utkin, J. Guldner, and J. Shi, *Sliding Modes in Electromechanical Systems*. London: Taylor and Francis, 1999.

[8] C. Edwards and S. Spurgeon, *Sliding Mode Control*. London: Taylor and Francis, 1998.

[9] S. Drakunov, U. Ozguner, P. Dix, and B. Ashrafi, "Abs control using optimum search via sliding modes," *IEEE Trans. on Control Systems Technology*, vol. 3, pp. 79–85, 1995.

[10] J. Ackermann, J. Guldner, R. Steinhausner, and V. I. Utkin, "Linear and nonlinear design for robust automatic steering," *IEEE Trans. on Control System Technology*, vol. 3, p. 132143, 1995.

[11] N. MSirdi, A. Rabhi, L. Fridman, J. Davila, and Y. Delanne, "Second order sliding-mode observer for estimation of vehicle dynamic parameters," *Int. J. Vehicle Design*, vol. 48, 2008.

[12] H. Shraim, M. Ouladsine, L. Fridman, and M. Romero, "Vehicle parameter estimation and stability enhancement using sliding modes techniques," *Int. J. Vehicle Design*, vol. 48, 2008.

[13] H. Imine and L. Fridman, "Road profile estimation in heavy vehicle dynamics simulation," *Int. J. Vehicle Design*, vol. 47, 2008.

[14] M. Amodeo, A. Ferrara, R. Terzaghi, and C. Vecchio, "Wheel slip control via second-order sliding-mode generation," *IEEE Transactions on Intelligent Transportation Systems*, vol. 11, pp. 122–130, 2010.

[15] A. Levant, "Higher-order sliding modes, differentiation and output-feedback control," *Int. J. of Control*, vol. 76, pp. 924–941, 2003.

[16] U. Kiencke and L. Nielsen, *Automotive Control Systems. For Engine, Driveline, and Vehicle*. Springer Verlag, 2005.

[17] A. Filippov, *Differential equations with discontinuous right hand-sides, Mathematics and its applications*. Kluwer Academic Publisher, 1988.

[18] L. Fridman and A. Levant, "Accuracy of homogeneous sliding modes in the presence of fast actuators," *IEEE Trans. on Automatic Control*, vol. 55, 2010.